



Outcomes of Partial Slip on Double-Diffusive Convection on Peristaltic Waves of Johnson–Segalman Nanofluids Under the Impact of Inclined Magnetic Field

Khalid Saeed¹ · Safia Akram² · Adeel Ahmad¹

Received: 21 March 2022 / Accepted: 15 February 2023 / Published online: 14 March 2023
© King Fahd University of Petroleum & Minerals 2023

Abstract

The outcomes of partial slip on double-diffusive convection of Johnson–Segalman nanofluids in an asymmetric peristaltic path are presented in this research with the effect of inclined magnetic field. The mathematical formulation of Johnson–Segalman nanofluids is also discussed with double-diffusive convection and inclined magnetic field. To simplify extremely nonlinear partial differential equations, a lubricant approach is applied. The numerical calculations are obtained to the equations for the stream function, concentration, pressure gradient, temperature, velocity, nanoparticle volume fraction, and pressure rise. The impact of prominent hydro-mechanical parameters such as Brownian motion, thermophoresis, Soret, Dufour, and slip constraints on the axial velocity, trapping, volumetric fraction, pressure gradient, temperature, pressure rise, and concentration functions is evaluated graphically. It is noted that slip effect in the channel causes the fluid particles to stray, slowing the fluid velocity. Moreover, it has been noted that as thermophoretic effects and Brownian motion increase, nanoparticles rapidly move from the wall into the fluid, significantly raising temperature.

Keywords Double-diffusive convection · Nanofluids · Partial slip · Peristaltic wave · Inclined magnetic field · Asymmetric channel · Johnson–Segalman fluid

List of symbols

C	Solutal concentration
T	Temperature
G_{rF}	Grashof number of nanoparticles
Ω	Nanoparticle volume fraction
D_B	Brownian diffusion coefficient
Re	Reynolds number
D_s	Solutal diffusivity
N_t	Thermophoresis parameter
$(\rho c)_f$	Heat capacity of fluid
N_{CT}	Soret parameter
G_{rc}	Solutal Grashof number
M	Hartmann number
Pr	Prandtl number
Le	Lewis number

N_b	Brownian motion parameter
D_T	Thermophoretic diffusion coefficient
G_{rt}	Thermal Grashof number
N_{TC}	Dufour parameter
Ln	Nanofluid Lewis number
$(\rho c)_p$	Heat capacity of nanoparticle
D_{TC}	Dufour diffusivity
D_{CT}	Soret diffusivity

Small alphabets

u	Axial velocity
g	Acceleration due to gravity
d_1, d_3	Channel width
k	Thermal conductivity
d_2, d_4	Wave amplitudes
v	Transverse velocity
b	Wave amplitude
p	Pressure
t	Time
c	Propagation of velocity

✉ Safia Akram
drsafiaakram@gmail.com; drsafiaakram@mcs.edu.pk

¹ Comsats University, Islamabad, Pakistan

² MCS, National University of Sciences and Technology, Islamabad, Pakistan



Greek symbols

δ	Wavelength
ρ_p	Nanoparticle mass density
γ	Solutal concentration
β_T	Volumetric coefficient of thermal expansion
ω_3	Concentration slip parameter
ω_1	Velocity slip parameter
δ	Wave number
Ψ	Stream function
$(\rho c)_p$	Nanoparticle heat capacity
Γ	Magnetic field inclination angle
β_C	Volumetric coefficient of solutal expansion
ω_4	Nanoparticles slip parameter
ω_2	Temperature slip parameter
Θ	Temperature

1 Introduction

The transportation of fluids caused by the constant contraction and relaxation of a channel is commonly known as peristalsis [1]. Such motion has diverse applications in different fields of modern era, in the human/animal body, motion of physiological fluids in vessels (like intestines, ureter, stomach, etc.) and blood vessels (like capillaries, veins, arteries, etc.). Other applications include urine moving to bladder from kidneys [2], motion of food through the esophagus, chime moving in the intestines, intrauterine unsolidified motion, and spermatozoa flow in ductus efferentes of masculine reproductive system. Similarly, motion by ovum in feminine uterine tube, transfer of lymph in veins, and vasomotion of arterioles, capillaries, and venules also follow the motion of peristaltic. In the field of bio-locomotion, the same analogy of peristalsis can be found in earthworms as an outer motion doing geonautical mobility very efficiently supported by the excretion of lubricating mucus. In addition, the same phenomenon is being followed in soil sciences where air is being forced through burrows [3]. Roller/finger pumps also work on this phenomenon, and besides, modern micro- and nanorobots are principally based on mechanisms of peristaltic [4]. Since the major investigation by Latham [5], many theoretical as well as experimental contributions are being made in research to understand the peristaltic flows in different scenarios. A review of the basic literature can be viewed in Jaffrin and Shapiro [6]. Burns and Parkes theoretically studied the peristaltic motion in [7]. Work by Chow [8], Mishra and Rao [9], Shapiro et al. [10], and Takabatake and Ayukawa [11] has motivated some interest in recent years. However, scope of these studies is limited to Newtonian fluids.

The famous Navier–Stokes equations are unable to describe the flow characteristics of many complex fluids such

as suspensions, liquid detergents, oils, drilling muds, and grease. Several researchers addressed this difficulty by suggesting diversified non-Newtonian fluid models. But, then these mathematical models raise the challenge of solving highly nonlinear and much more complicated when compared with the Navier–Stokes model. One such model is named as Johnson–Segalman model which is suitable for viscoelastic flows and designed to tolerate non-affine deformation [12]. This model has distinct characteristic when compared to other fluid models in the sense that for simple shear flow, it permits non-monotonic change in shear stress with the increase (decrease) in the rate of deformation. Some non-Newtonian fluids possess an exciting property called spurt. It refers to an abnormal rise in volume for a small rise in pressure gradient. Spurt occurrence based on the above-mentioned non-monotonic change is discussed in detail in [13–17].

The term "nanofluid" refers to a type of fluids in which nanoparticles are uniformly disseminated throughout the base fluid, such as water, oil, and ethylene glycol. Nanofluids gained enormous attention in start of twenty-first century. Even after two decades of this century, these fluids are still a source of attention for various researchers as these have strong effects on related flow characteristics in various areas of interest. Choi [18] was first one, who proposed nanofluids. Experimental as well as theoretical studies show that nanofluids improve thermo-physical properties when compared with ordinary fluids. Nanoparticles have random motion, often called Brownian motion, in liquids and possibly collide in nanofluids. Collision is suggested to be one possible reason for enhancement of thermal conductivity. Nanofluids when associated with peristalsis have important applications in medical field including cancer treatment and drug delivery, chemical engineering including chemicals transportation, and mechanical engineering field. In recent times, such a collective study of peristalsis and nanofluids [19–25] has been modeled for physiological flows to examine the effects of nanofluids on peristaltic motion.

The study of the influence of magnetic force in peristaltic transport is crucial from a biological perspective. Physiological fluids include biomagnetic fluids as a subpart. Furthermore, investigation of magnetohydrodynamics (MHD) in biomagnetic flows has an immense importance in medicinal field. Some examples include observing the blood flow rates, magnetic equipment for cell separation, and evaluating strong magnetic field effects on the cardiovascular system. Considering these wide ranges of applications, many researchers have studied the MHD of biomagnetic flow under various considerations [26–28]. Electrical machines performing magnetic resonance imaging (MRI) tests are based on similar idea. Also, magnetic field in the presence of nanofluid plays a major role in medical applications like cancer therapy and existing medication distribution (Tripathi



and Beg [29]). Nanofluids made of titanium nanoparticles are used to treat cancer patients by radiation having magnetic attributes destroying tumor cells without damaging strong tissues. Knowing the physical importance of nanofluids with magnetism, Sucharitha et al. [30] studied the MHD flow of nanofluid in a non-uniform channel with effects of Joule heating. Some important contributions are made in research on nanofluids, taking thermophoresis effects with Brownian motion to study motion [31–40].

Double-diffusion phenomena refer to the mixing of fluids with two constituents with distinct molecular diffusivities. Such phenomena are observed in oceanography, solid-state physics, astrophysics, chemical processes, biology, and geophysics [41]. Also, in industries, solar ponds, crystal manufacturing, storage tanks of natural gas, and metal solidification processes double diffusion is observed. Some researchers have used double-diffusive convection in analyzing peristaltic movement. The same effects in the presence of nanofluid were analyzed in [42] by Noreen et al. More research work can be found on double diffusion in [20, 43–48].

In most of the early work on peristalsis, no-slip conditions are used to study the flow. However, effects of slip condition are always of interest in applied sciences due to their practical applications. Combination of both slip conditions and nanoparticles is of great interest for researchers because of their key role thermal systems utilized by industries. Slip effect is based on such a motion in which velocity of particles is perturbed adjacent to the surface/boundary. Navier established the idea of the slip phenomenon, which states that shear stress and fluid velocity rate near the surface are proportional. Afterward, the concept of partial slip on boundaries was investigated by several researchers with various fluid models and different geometries [49–54].

The effects of multiple slip conditions on the peristaltic flow with magnetic field for Johnson–Segalman nanofluid incorporating double-diffusive convection are considered for the present problem. To the best of our knowledge, such combination was not studied for Johnson–Segalman nanofluids before. Such a combination can provide basis for further theoretical and practical research in drug delivery systems. Effects of various parameters on bolus formation in the flow may also be utilized in diseases management. Also, consideration of electromagnetic waves expands the horizon of the study to the application in cancer therapy as well. This study will help in assessment of chyme movement in the gastrointestinal tract and in regulating the intensity of magnetic field of the blood flow during surgery.

2 Basic Equations

The basic equations of incompressible Johnson–Segalman nanofluids are defined as follows [44]:

The continuity equation for the incompressible fluid is defined as

$$\text{div} V = 0, \tag{1}$$

Navier–Stoke equation is defined as

$$\rho_f \left(\frac{dV}{dt} \right) = \text{div} \tau + \rho f + g \{ (1 - \Theta_0) \rho_{f0} \{ \beta_T (T - T_0) + \beta_C (C - C_0) \} - (\rho_p - \rho_{f0}) (\Theta - \Theta_0) \}, \tag{2}$$

The energy equation is defined as

$$(\rho c)_f \left(\frac{dT}{dt} \right) = k \nabla^2 T + (\rho c)_p \{ D_B (\nabla \Theta \cdot \nabla T) + \left(\frac{D_T}{T_0} \right) \nabla T \cdot \nabla T \} + D_{TC} \nabla^2 C, \tag{3}$$

The solute concentration is defined as

$$\frac{dC}{dt} = D_s \nabla^2 C + D_{CT} \nabla^2 T, \tag{4}$$

The nanoparticle fraction equation is defined as

$$\frac{d\Theta}{dt} = D_B \nabla^2 \Theta + \left(\frac{D_T}{T_0} \right) \nabla^2 T, \tag{5}$$

where ρ_f denotes the base fluid density, V stands for the velocity vector, τ is the stress tensor, d/dt represents the derivative of material time, g stands for the acceleration, f denotes the body force, ρ_{f0} is the fluid density at T_0 , ρ_p denotes the particles density, T denotes the temperature, C is the concentration, D_T is the thermophoretic diffusion, Θ stands for the nanoparticle volume fraction, D_B is the Brownian diffusion, D_{CT} is the Soret diffusively, D_s is the solutal diffusively, D_{TC} is the Dufour diffusively, β_C is the volumetric solutal expansion coefficient of a fluid, β_T is the volumetric thermal expansion coefficient of a fluid, k is the thermal conductivity, $(\rho c)_p$ is the heat capacity of nanoparticle, and $(\rho c)_f$ stands for the fluid heat capacity.

The Johnson–Segalman fluid stress tensor is defined by [16]

$$\tau = -PI + \sigma, \tag{6}$$

$$\sigma = 2\mu D + S, \tag{7}$$

$$S + \xi \left[\frac{dS}{dt} + S(W - \beta D) + (W - \beta D)^T S \right] = 2\eta D, \quad (8)$$

$$D = \frac{1}{2}(\text{grad}(V) + \text{grad}(V)^*), \quad (9)$$

$$W = \frac{1}{2}(\text{grad}(V) - \text{grad}(V)^*), \quad (10)$$

where P , I , (μ, η) , ξ , β , D , and W denote the pressure, identity tensor, dynamic viscosities, relaxation time, slip parameter, velocity gradient symmetric, and skew symmetric part, respectively. Note that model (6) reduces to the Maxwell fluid model for $\beta = 1$ and $\mu = 0$, and for $\mu = 0 = \xi$, we receive the classical Navier–Stokes fluid model.

3 Mathematical Formulation

Let us consider Johnson–Segalman fluid nanofluid and examined the flow within condensed, electrically confined dual dimensional conduit with a diameter of $d_1 + d_2$. Cartesian coordinates are drawn by keeping the center of channel at X -axis and cross-sectional region on Y -axis. The sinusoidal wave moves smoothly on the wall along the channel. The values of temperatures, solvent concentrations, and nanoparticle fraction are calculated as $T = T_0$, $C = C_0$, $\Theta = \Theta_0$, (at $y = H_1$), and $T = T_1$, $C = C_1$, $\Theta = \Theta_1$ (at $y = H_2$). Magnetic flux remained constant at an angle Γ . Magnetic Reynolds number is kept very low, while electric field is taken as null. Resultantly, induced magnetic flux is not considerable in comparison with applied magnetic flux.

The geometrical shape is defined in Fig. 1, and mathematical expression of geometry of problem is defined as [16]

$$Y = d_1 + d_3 \cos\left(\frac{2\pi}{\lambda}(X - ct)\right) = H_1, \\ Y = -d_2 - d_4 \cos\left(\frac{2\pi}{\lambda}(X - ct) + \varphi\right) = H_2, \quad (11)$$

where c denotes the wave of speed, t stands for the time, (d_3, d_4) represents the wave amplitudes, (d_1, d_2) stands for the channel width, λ denotes the wavelength, and φ stands for the phase difference with a range of $0 \leq \varphi \leq \pi$. At $\varphi = 0$, channel is symmetric with out-of-phase waves and $\varphi = \pi$ represents a channel with a phase wave. Moreover, wave amplitudes (d_3, d_4) , channel width (d_1, d_2) , and phase difference φ satisfy the following criterion $d_4^2 + d_3^2 + 2d_3d_4 \cos \varphi \leq (d_1 + d_2)^2$.

Velocity for two-dimensional and directional flow is

$$V = (U(X, Y, t), V(X, Y, t), 0). \quad (12)$$

Using Eq. (12), Eqs. (1)–(10) become

$$\frac{\partial U}{\partial X} + \frac{\partial V}{\partial Y} = 0, \quad (13)$$

$$\rho \left(\frac{\partial}{\partial t} + U \frac{\partial}{\partial X} + V \frac{\partial}{\partial Y} \right) U = -\frac{\partial P}{\partial X} + \mu \left(\frac{\partial^2 U}{\partial X^2} + \frac{\partial^2 U}{\partial Y^2} \right) \\ + \frac{\partial S_{XX}}{\partial X} + \frac{\partial S_{XY}}{\partial Y} - \sigma B_0^2 \cos \Gamma (U \cos \Gamma - V \sin \Gamma) \\ + g \{ (1 - \Theta_0) \rho_{f0} \{ \beta_T (T - T_0) + \beta_C (C - C_0) \} \\ - (\rho_p - \rho_{f0}) (\Theta - \Theta_0) \}, \quad (14)$$

$$\rho \left(\frac{\partial}{\partial t} + U \frac{\partial}{\partial X} + V \frac{\partial}{\partial Y} \right) V = -\frac{\partial P}{\partial Y} + \mu \left(\frac{\partial^2 V}{\partial X^2} + \frac{\partial^2 V}{\partial Y^2} \right) \\ + \frac{\partial S_{YX}}{\partial X} + \frac{\partial S_{YY}}{\partial Y} \\ + \sigma B_0^2 \sin \Gamma (U \cos \Gamma - V \sin \Gamma), \quad (15)$$

$$(\rho c) f \left(\frac{\partial}{\partial t} + U \frac{\partial}{\partial X} + V \frac{\partial}{\partial Y} \right) T = k \left(\frac{\partial^2 T}{\partial X^2} + \frac{\partial^2 T}{\partial Y^2} \right) + (\rho c) p \\ \times \left\{ D_B \left(\frac{\partial \Theta}{\partial X} \frac{\partial T}{\partial X} + \frac{\partial \Theta}{\partial Y} \frac{\partial T}{\partial Y} \right) \right. \\ \left. \left(\frac{D_T}{T_0} \right) \left[\left(\frac{\partial T}{\partial X} \right)^2 + \left(\frac{\partial T}{\partial Y} \right)^2 \right] \right\} \\ + D_{TC} \left(\frac{\partial^2 C}{\partial X^2} + \frac{\partial^2 C}{\partial Y^2} \right), \quad (16)$$

$$\left(\frac{\partial}{\partial t} + U \frac{\partial}{\partial X} + V \frac{\partial}{\partial Y} \right) C = D_s \left(\frac{\partial^2 C}{\partial X^2} + \frac{\partial^2 C}{\partial Y^2} \right) \\ + D_{TC} \left(\frac{\partial^2 T}{\partial X^2} + \frac{\partial^2 T}{\partial Y^2} \right), \quad (17)$$

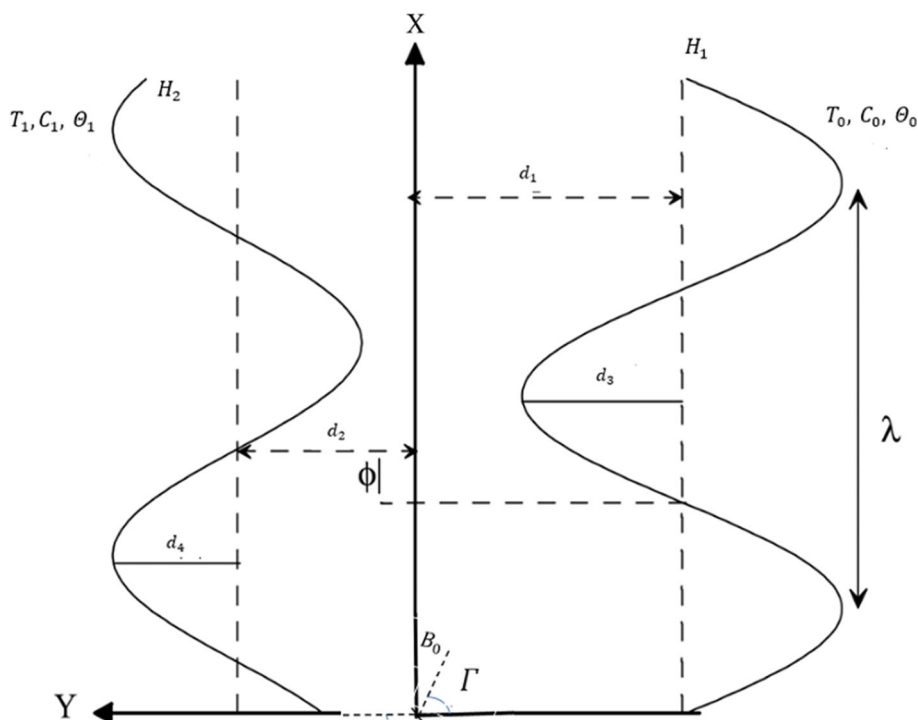
$$\left(\frac{\partial}{\partial t} + U \frac{\partial}{\partial X} + V \frac{\partial}{\partial Y} \right) \Theta = D_B \left(\frac{\partial^2 \Theta}{\partial X^2} + \frac{\partial^2 \Theta}{\partial Y^2} \right) \\ + \left(\frac{D_T}{T_0} \right) \left(\frac{\partial^2 T}{\partial X^2} + \frac{\partial^2 T}{\partial Y^2} \right), \quad (18)$$

$$2\eta \frac{\partial U}{\partial X} = S_{XX} + \xi \left(\frac{\partial}{\partial t} + U \frac{\partial}{\partial X} + V \frac{\partial}{\partial Y} \right) S_{XX} - 2\xi \beta S_{XX} \frac{\partial U}{\partial X} \\ + \xi \left[(1 - \beta) \frac{\partial V}{\partial X} - (1 + \beta) \frac{\partial U}{\partial Y} \right] S_{XY}, \quad (19)$$

$$\eta \left(\frac{\partial U}{\partial Y} + \frac{\partial V}{\partial X} \right) = S_{XY} + \xi \left(\frac{\partial}{\partial t} + U \frac{\partial}{\partial X} + V \frac{\partial}{\partial Y} \right) S_{XY} \\ + \frac{\xi}{2} \left[(1 - \beta) \frac{\partial U}{\partial Y} - (1 + \beta) \frac{\partial V}{\partial X} \right] S_{XX} \\ + \frac{\xi}{2} \left[(1 - \beta) \frac{\partial V}{\partial X} - (1 + \beta) \frac{\partial U}{\partial Y} \right] S_{YY}, \quad (20)$$



Fig. 1 Geometrical shape of the walls



$$2\eta \frac{\partial V}{\partial Y} = S_{YY} + \xi \left(\frac{\partial}{\partial t} + U \frac{\partial}{\partial X} + V \frac{\partial}{\partial Y} \right) S_{YY} - 2\xi\beta S_{YY} \frac{\partial V}{\partial Y} + \xi \left[(1 - \beta) \frac{\partial U}{\partial Y} - (1 + \beta) \frac{\partial V}{\partial X} \right] S_{XY}. \quad (21)$$

Now introduce Galilean transformations in fixed frame (X, Y) and wave frame (x, y) as

$$v = V, u = U - c, y = Y, x = X - ct, p(x, y) = P(X, Y, t), \quad (22)$$

and define non-dimensional parameters [16, 47, 48]

$$\begin{aligned} \bar{v} &= \frac{v}{c}, \bar{x} = \frac{x}{\lambda}, \bar{u} = \frac{u}{c}, \bar{y} = \frac{y}{d_1}, \delta = \frac{d_1}{\lambda}, \bar{t} = \frac{ct}{\lambda}, \\ d &= \frac{d_2}{d_1}, h_2 = \frac{H_2}{d_2}, b = \frac{d_4}{d_1}, h_1 = \frac{H_1}{d_1}, a = \frac{d_3}{d_1}, \\ \bar{p} &= \frac{d_1^2 p(x)}{(\mu + \eta)c\lambda}, Pr = \frac{(\rho c)_f v}{k}, \\ Re &= \frac{\rho_f c d_1}{\mu}, v = \frac{\mu}{\rho_f}, Le = \frac{v}{D_s}, \\ Ln &= \frac{v}{D_B}, v = -\delta \frac{\partial \psi}{\partial x}, u = \frac{\partial \psi}{\partial y}, \\ G_{rc} &= \frac{g(1 - \Theta_0)\rho_{f0}\beta_c(C_1 - C_0)d_1^2}{\mu c}, \\ G_{rF} &= \frac{g(\rho_p - \rho_{f0})(\Theta_1 - \Theta_0)}{\mu c} d_1^2, \end{aligned}$$

$$\begin{aligned} N_t &= \frac{(\rho c)_p D_T (T_1 - T_0)}{T_0 k}, \\ \theta &= \frac{T - T_0}{T_1 - T_0}, \gamma = \frac{C - C_0}{C_1 - C_0}, \Omega = \frac{\Theta - \Theta_0}{\Theta_1 - \Theta_0}, \\ Wi &= \frac{c\xi}{d_1}, \bar{S} = \frac{d_1}{\mu c} S, N_{CT} = \frac{D_{CT}(T_1 - T_0)}{(C_1 - C_0)D_s}, \\ N_{TC} &= \frac{D_{CT}(C_1 - C_0)}{k(T_1 - T_0)}, \\ G_{rt} &= \frac{g d_1^2 (1 - \Theta_0)(T_1 - T_0)\rho_{f0}\beta_T}{\mu c}, \\ N_b &= \frac{(\rho c)_p D_B (\Theta_1 - \Theta_0)}{k}, \\ M &= \sqrt{\frac{\sigma}{\mu}} B_0 d_1, \end{aligned} \quad (23)$$

where $\theta, \delta, \gamma, N_b, Re, G_{rF}, Pr, Le, G_{rt}, G_{rc}, N_{CT}, Ln, N_t, \Omega, N_{TC}, \mu, k$ represent the temperature, wave number, solutal (species) concentration, Brownian motion, Reynolds number, nanoparticle Grashof number, Prandtl number, Lewis number, thermal Grashof number, solutal Grashof number, Soret parameter, nanofluid Lewis number, thermophoresis parameter, nanoparticle fraction, Dufour parameter, viscosity of fluid, and thermal conductivity, respectively.

Equation (5) is satisfied automatically using Eqs. (12) and (13), and Eqs. (6) to (10) in the wave frame (by dropping bars) become

$$Re\delta(\psi_{xy}\psi_y - \psi_{yy}\psi_x) = -\left(\frac{\mu + \eta}{\mu}\right) \frac{\partial p}{\partial x} + \delta \frac{\partial S_{xx}}{\partial x}$$

$$\begin{aligned} & + \frac{\partial S_{xy}}{\partial y} + \left(\delta^2 \frac{\partial^3 \psi}{\partial x^2 \partial y} + \frac{\partial^3 \psi}{\partial y^3} \right) \\ & - M^2 \cos \Gamma ((\psi_y + 1) \cos \Gamma + \delta \psi_x \sin \Gamma) \\ & + G_{rt} \theta + G_{rc} \gamma - G_{rF} \Omega, \end{aligned} \quad (24)$$

$$\begin{aligned} \text{Re } \delta^3 (\psi_{xy} \psi_x - \psi_{xx} \psi_y) &= - \left(\frac{\mu + \eta}{\mu} \right) \frac{\partial p}{\partial y} \\ & + \delta^2 \frac{\partial S_{xy}}{\partial x} + \delta \frac{\partial S_{yy}}{\partial y} - \delta^2 \left(\delta^2 \frac{\partial^3 \psi}{\partial x^3} + \frac{\partial^3 \psi}{\partial x \partial y^2} \right) \\ & + M^2 \delta \sin \Gamma ((\psi_y + 1) \cos \Gamma + \psi_x \delta \sin \Gamma), \end{aligned} \quad (25)$$

$$\begin{aligned} \text{Re } Pr \delta (\theta_x \psi_y - \theta_y \psi_x) &= (\theta_{yy} + \delta^2 \theta_{xx}) \\ & + N_{TC} (\delta^2 \gamma_{xx} + \gamma_{yy}) \\ & + N_b (\delta^2 \Omega_x \theta_x + \theta_y \Omega_y) \\ & + N_t (\delta^2 (\theta_x)^2 + (\theta_y)^2), \end{aligned} \quad (26)$$

$$\begin{aligned} \text{Re } \delta Le (\gamma_x \psi_y - \gamma_y \psi_x) &= (\delta^2 \gamma_{xx} + \gamma_{yy}) \\ & + N_{CT} (\delta^2 \theta_{xx} + \theta_{yy}), \end{aligned} \quad (27)$$

$$\begin{aligned} \text{Re } \delta Ln (\psi_y \Omega_x - \psi_x \Omega_y) &= (\delta^2 \Omega_{xx} + \Omega_{yy}) \\ & + \frac{N_t}{N_b} (\delta^2 \theta_{xx} + \theta_{yy}), \end{aligned} \quad (28)$$

$$\begin{aligned} \left(\frac{2\delta\eta}{\mu} \right) \frac{\partial^2 \psi}{\partial x \partial y} &= S_{xx} + \delta Wi \left(\frac{\partial \psi}{\partial y} \frac{\partial}{\partial x} - \frac{\partial \psi}{\partial x} \frac{\partial}{\partial y} \right) S_{xx} \\ & - 2\beta Wi \delta \frac{\partial^2 \psi}{\partial x \partial y} \\ & - Wi \left(\delta^2 (1 - \beta) \frac{\partial^2 \psi}{\partial x^2} + (1 + \beta) \frac{\partial^2 \psi}{\partial y^2} \right) S_{xy}, \end{aligned} \quad (29)$$

$$\begin{aligned} \frac{\eta}{\mu} \left(\frac{\partial^2 \psi}{\partial y^2} - \delta^2 \frac{\partial^2 \psi}{\partial x^2} \right) &= S_{xy} + Wi \delta \left(\frac{\partial \psi}{\partial y} \frac{\partial}{\partial x} - \frac{\partial \psi}{\partial x} \frac{\partial}{\partial y} \right) S_{xy} \\ & + \frac{Wi}{2} \left((1 - \beta) \frac{\partial^2 \psi}{\partial y^2} + \delta^2 (1 + \beta) \frac{\partial^2 \psi}{\partial x^2} \right) S_{xx} \\ & - \frac{Wi}{2} \left(\delta^2 (1 - \beta) \frac{\partial^2 \psi}{\partial x^2} + (1 + \beta) \frac{\partial^2 \psi}{\partial y^2} \right) S_{yy}, \end{aligned} \quad (30)$$

$$\begin{aligned} - \left(\frac{2\delta\eta}{\mu} \right) \frac{\partial^2 \psi}{\partial x \partial y} &= S_{yy} + Wi \delta \left(\frac{\partial \psi}{\partial y} \frac{\partial}{\partial x} - \frac{\partial \psi}{\partial x} \frac{\partial}{\partial y} \right) S_{yy} \\ & + 2\beta \delta Wi \frac{\partial^2 \psi}{\partial x \partial y} S_{yy} \\ & + Wi \left((1 - \beta) \frac{\partial^2 \psi}{\partial y^2} + \delta^2 (1 + \beta) \frac{\partial^2 \psi}{\partial x^2} \right) S_{xy}. \end{aligned} \quad (31)$$

Using lubricant approach ($\delta \ll 1$, $\text{Re} \rightarrow 0$), Eqs. (14) to (18) are now reduced as

$$\begin{aligned} 0 &= - \left(\frac{\mu + \eta}{\mu} \right) \frac{\partial p}{\partial x} + \frac{\partial S_{xy}}{\partial y} + \frac{\partial^3 \psi}{\partial y^3} \\ & - M^2 \cos^2 \Gamma \left(\frac{\partial \psi}{\partial y} + 1 \right) + G_{rt} \theta + G_{rc} \gamma - G_{rF} \Omega, \end{aligned} \quad (32)$$

$$0 = - \frac{\partial p}{\partial y}, \quad (33)$$

$$\frac{\partial^2 \theta}{\partial y^2} + N_{TC} \frac{\partial^2 \gamma}{\partial y^2} + N_b \left(\frac{\partial \Omega}{\partial y} \frac{\partial \theta}{\partial y} \right) + N_t \left(\frac{\partial \theta}{\partial y} \right)^2 = 0, \quad (34)$$

$$\frac{\partial^2 \gamma}{\partial y^2} + N_{CT} \frac{\partial^2 \theta}{\partial y^2} = 0, \quad (35)$$

$$\frac{\partial^2 \Omega}{\partial y^2} + \frac{N_t}{N_b} \frac{\partial^2 \theta}{\partial y^2} = 0, \quad (36)$$

where

$$S_{xx} = Wi(1 + \beta) \frac{\partial^2 \psi}{\partial y^2} S_{xy}, \quad (37)$$

$$\left(\frac{\eta}{\mu} \right) \frac{\partial^2 \psi}{\partial y^2} = S_{xy} + \frac{Wi}{2} (1 - \beta) \frac{\partial^2 \psi}{\partial y^2} S_{xx} - \frac{Wi}{2} (1 + \beta) \frac{\partial^2 \psi}{\partial y^2} S_{yy}, \quad (38)$$

$$S_{yy} = -Wi(1 - \beta) \frac{\partial^2 \psi}{\partial y^2} S_{xy}. \quad (39)$$

Now reducing pressure from Eqs. (19) and (20) and using Eq. (24), we now have the following expression:

$$\begin{aligned} \frac{\partial^2 S_{xy}}{\partial y^2} + \frac{\partial^4 \psi}{\partial y^4} - M^2 \cos^2 \Gamma \frac{\partial^2 \psi}{\partial y^2} \\ + G_{rt} \frac{\partial \theta}{\partial y} + G_{rc} \frac{\partial \gamma}{\partial y} - G_{rF} \frac{\partial \Omega}{\partial y} = 0, \end{aligned} \quad (40)$$

$$S_{xy} = \frac{\left(\frac{\eta}{\mu} \right) \left(\frac{\partial^2 \psi}{\partial y^2} \right)}{1 + Wi^2 (1 - \beta^2) \left(\frac{\partial^2 \psi}{\partial y^2} \right)^2}, \quad (41)$$

$$\frac{\partial^2}{\partial y^2} \left[\frac{\left(\frac{\eta}{\mu} + 1\right) \left(\frac{\partial^2 \psi}{\partial y^2}\right) + Wi^2(1 - \beta^2) \left(\frac{\partial^2 \psi}{\partial y^2}\right)^3}{1 + Wi^2(1 - \beta^2) \left(\frac{\partial^2 \psi}{\partial y^2}\right)^2} \right] - M^2 \cos^2 \Gamma \frac{\partial^2 \psi}{\partial y^2} + G_{rt} \frac{\partial \theta}{\partial y} + G_{rc} \frac{\partial \gamma}{\partial y} - G_{rF} \frac{\partial \Omega}{\partial y} = 0. \tag{42}$$

$$\left(\frac{\mu + \eta}{\eta}\right) \frac{\partial p}{\partial x} = \frac{\partial}{\partial y} \left(\frac{\partial^2 \psi}{\partial y^2}\right) \left[\frac{\frac{\eta}{\mu} \left(\frac{\partial^2 \psi}{\partial y^2}\right)}{1 + Wi^2(1 - \beta^2) \left(\frac{\partial^2 \psi}{\partial y^2}\right)} \right] + \frac{\partial^3 \psi}{\partial y^3} - M^2 \cos^2 \Gamma \left(\frac{\partial \psi}{\partial y} + 1\right) + G_{rt} \theta + G_{rc} - G_{rF} \Omega \tag{43}$$

After using binomial expansion for small Wi^2 , Eqs. (42) and (43) may be simplified to

$$\frac{\partial^2}{\partial y^2} \left[\frac{\partial^2 \psi}{\partial y^2} + Wi^2 \lambda_1 \left(\frac{\partial^2 \psi}{\partial y^2}\right)^3 + Wi^4 \lambda_2 \left(\frac{\partial^2 \psi}{\partial y^2}\right)^5 \right] - M^2 \cos^2 \Gamma \frac{\partial^2 \psi}{\partial y^2} + G_{rt} \frac{\partial \theta}{\partial y} + G_{rc} \frac{\partial \gamma}{\partial y} - G_{rF} \frac{\partial \Omega}{\partial y} = 0, \tag{44}$$

$$\frac{\partial p}{\partial x} = \frac{\partial^3 \psi}{\partial y^3} + Wi^2 \lambda_1 \frac{\partial}{\partial y} \left[\left(\frac{\partial^2 \psi}{\partial y^2}\right)^3 \right] + Wi^4 \lambda_2 \frac{\partial}{\partial y} \left[\left(\frac{\partial^2 \psi}{\partial y^2}\right)^5 \right] - M^2 \cos^2 \Gamma (\psi_y + 1) + G_{rt} \theta + G_{rc} \gamma - G_{rF} \Omega, \tag{45}$$

$$\lambda_1 = \frac{(\beta^2 - 1)\eta}{(\eta + \mu)}, \lambda_2 = (\beta^2 - 1)\lambda_1. \tag{46}$$

In wave frame, the boundary conditions for the initiate problem are given as

$$\psi = \frac{F}{2}, \text{ at } y = h_1(x),$$

$$\psi = -\frac{F}{2}, \text{ at } y = h_2(x),$$

$$\frac{\partial \psi}{\partial y} + \omega_1 \left(\frac{\partial^2 \psi}{\partial y^2} + S_{xy}\right) = -1 \text{ on } y = h_1(x),$$

$$\frac{\partial \psi}{\partial y} - \omega_1 \left(\frac{\partial^2 \psi}{\partial y^2} + S_{xy}\right) = -1 \text{ on } y = h_2(x),$$

$$\theta + \omega_2 \frac{\partial \theta}{\partial y} = 0, \text{ on } y = h_1(x), \tag{47}$$

$$\theta - \omega_2 \frac{\partial \theta}{\partial y} = 1, \text{ on } y = h_2(x), \tag{48}$$

$$\gamma + \omega_3 \frac{\partial \gamma}{\partial y} = 0, \text{ on } y = h_1(x),$$

$$\gamma - \omega_3 \frac{\partial \gamma}{\partial y} = 1, \text{ on } y = h_2(x), \tag{49}$$

$$\Omega + \omega_4 \frac{\partial \Omega}{\partial y} = 0, \text{ on } y = h_1(x),$$

$$\Omega - \omega_4 \frac{\partial \Omega}{\partial y} = 1, \text{ on } y = h_2(x). \tag{50}$$

If $\omega_1, \omega_2, \omega_3,$ and ω_4 in the above-mentioned conditions are all zero, there are no-slip conditions.

The mean flow Q is computed in dimensionless form as follows:

$$Q = F + 1 + d, \tag{51}$$

where

$$F = \int_{h_2(x)}^{h_1(x)} \frac{\partial \psi}{\partial y} dy = \psi(h_1(x)) - \psi(h_2(x)), \tag{52}$$

where

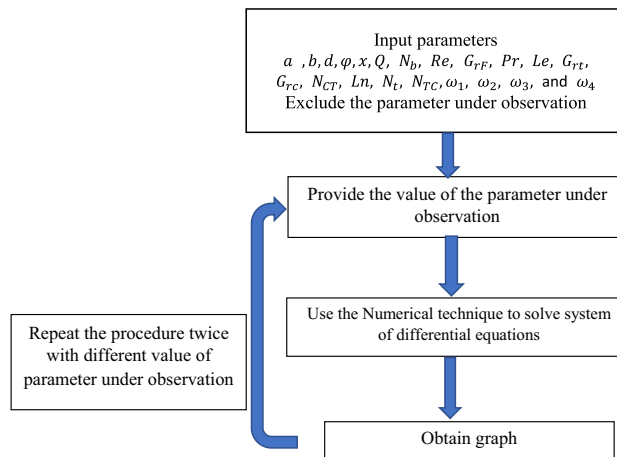
$$h_1(x) = 1 + a \cos 2\pi x, \quad h_2(x) = -d - b \cos(2\pi x + \varphi). \tag{53}$$

3.1 Special Case:

The results of [16] can also be retrieved as a special case of an existing problem in the absence of double-diffusive convection ($G_{rt} = 0 = G_{rc} = G_{rF}$), slip conditions ($\omega_1 = \omega_2 = \omega_3 = \omega_4 = 0$), and $M = 0$.

The results of [9] can also be retrieved as a special case of an existing problem in the absence of double-diffusive convection ($G_{rt} = 0 = G_{rc} = G_{rF}$), non-Newtonian fluid ($\lambda_1 = 0 = \lambda_2$), slip conditions ($\omega_1 = \omega_2 = \omega_3 = \omega_4 = 0$), and $M = 0$.

Flowchart: Flowchart showing the hierarchy of the ongoing problem



4 Numerical Solution and Validation

Due to nonlinearity of partial differential equations, finding exact solutions to Eqs. (21)–(25) is extremely challenging. Differential equations are solved using the NDSolve command in the MATHEMATICA software. This command is based on different types of numerical methods. Some of these methods are: Explicit Euler, midpoint rule method, midpoint rule method with Gragg smoothing, and linearly implicit Bader-smoothed midpoint rule method. Settings are kept at default in which equations are solved numerically by the best suitable method for solving the system of equations. Table 1 is generated to show the comparison of the present work with the available literature. It is depicted from Table 1 that in the absence of slip, the numerical solution satisfied the boundary conditions at $y = h_1(x)$ and $y = h_2(x)$ and our numerical results matches with Hayat et al. [16] and viscous fluid [4] in the absence of double-diffusive convection and slip parameter.

5 Results and Discussion

In this section, graphical depiction is achieved as a result of numerical computation to solutions. To analyze the importance of temperature on several parameters such as thermophoresis N_t , Brownian motion N_b , Soret N_{CT} , Dufour N_{TC} , and temperature slip ω_2 , Fig. 2a, b is plotted. As noticed in Fig. 2a and b, the temperature profile increases when thermophoresis N_t and Brownian motion N_b parameters are enhanced. Because of the rise in Brownian motion and thermophoretic effects, nanoparticles actively

travel from the wall toward the fluid, vastly increasing temperature. The similar behavior is noted for the case of Soret N_{CT} and Dufour N_{TC} parameters. The temperature profile shows its increasing behavior by enhancing values of N_{CT} and N_{TC} (Fig. 2c and d). To study the impact of partial slip parameter of temperature ω_2 , Fig. 2e is drawn. It is notable in Fig. 2e that temperature profile decreases in the zone when $y \in [-0.3, -0.1]$ but when $y \in [-0.1, 0.65]$ the temperature profile increases due to increasing values of temperature slip parameter ω_2 . Because of the slip, the kinetic energy between fluid particles increases, raising the fluid temperature (Fig. 2e). To explore the significance of concentration on thermophoresis N_t , Brownian motion N_b , Soret N_{CT} , Dufour N_{TC} , and slip parameter of concentration ω_3 , Fig. 3a–e is plotted. It is noted from Fig. 3a–e that the concentration profile decreases by enhancing thermophoresis N_t , Brownian motion N_b , Soret N_{CT} , Dufour N_{TC} , and slip constraint of concentration ω_3 . Figure 4a–e is displayed to examine the effect of nanoparticle fraction on several parameters such as thermophoresis N_t , Brownian motion N_b , Soret parameter N_{CT} , Dufour parameter N_{TC} , and slip parameter of nanoparticle fraction ω_4 . As shown in Fig. 4a, increasing Brownian motion N_b raises the density of nanoparticles fraction. Furthermore, in the cases of N_t , N_{CT} , N_{TC} , and ω_4 , opposite behavior is observed. By growing the values of N_{CT} , N_t , N_{TC} and ω_4 , the nanoparticle fraction drops (Fig. 4b–e). This is owing to the fact that when N_t grows, the fluid viscosity falls, resulting in a smaller volume fraction occupied by the less dense particles. Moreover, since the channel walls generate less disturbance to the fluid particles due to the slip effect, higher values of ω_4 cause the concentration to decrease. As a result, the mass transfer rate of nanoparticles is slowed. Figure 5a–f shows the changes in pressure rise (Δp) vs mean flow rate (Q) for multiple slip parameter β values, Weissenberg number Wi , Hartmann number M , velocity slip constraint ω_1 , thermophoresis N_t , and thermal Grashof number G_{rt} . It clearly shows that raising β , M , and Wi increases the pumping rate in the pumping region " $\Delta p > 0$ " and in free pumping region " $\Delta p = 0$ ". In the copumping region " $\Delta p < 0$ ", the pumping rate decreases when β , M , and Wi increase (Fig. 5a–c). The velocity slip constraint ω_1 has the opposite conduct on pressure rise when compared with β , M , and Wi (Fig. 5d). Here, pumping rate decreases in pumping zone " $\Delta p > 0$ " and in free pumping zone " $\Delta p = 0$ " by increasing velocity slip parameter ω_1 . The pumping rate increases in pumping region " $\Delta p > 0$ ", in free pumping region " $\Delta p = 0$ ", and in copumping region " $\Delta p < 0$ " by increasing N_t and G_{rt} values (Fig. 5e and f). Figure 6a and d reveals the deviations of dp/dx against x for different slip parameter β , Hartmann number M , Weissenberg number Wi , and thermophoresis N_t values. It is found that in broader parts of channel $x \in [0, 0.4]$ and $x \in [0.6, 1]$, the pressure gradient is comparatively small.

Table 1 Comparison with the available literature

$y = h(x)$	Velocity profile $u(x)$		
	Present work (With partial slip)	Hayat et al. [16] (Without partial slip)	Viscous fluid [9] (Without partial slip)
0.838187	−0.757689	−1	−1
0.710756	−0.68338	−0.815984	−0.799008
0.583325	−0.626128	−0.666764	−0.642681
0.455895	−0.585952	−0.553954	−0.531019
0.328464	−0.562874	−0.479416	−0.464021
0.201033	−0.55690	−0.445331	−0.441689
0.0736029	−0.568003	−0.454301	−0.464021
−0.0538277	−0.596102	−0.509511	−0.531019
−0.181258	−0.641041	−0.614975	−0.642681
−0.308689	−0.702576	−0.775989	−0.799008
−0.43612	−0.780348	−1	



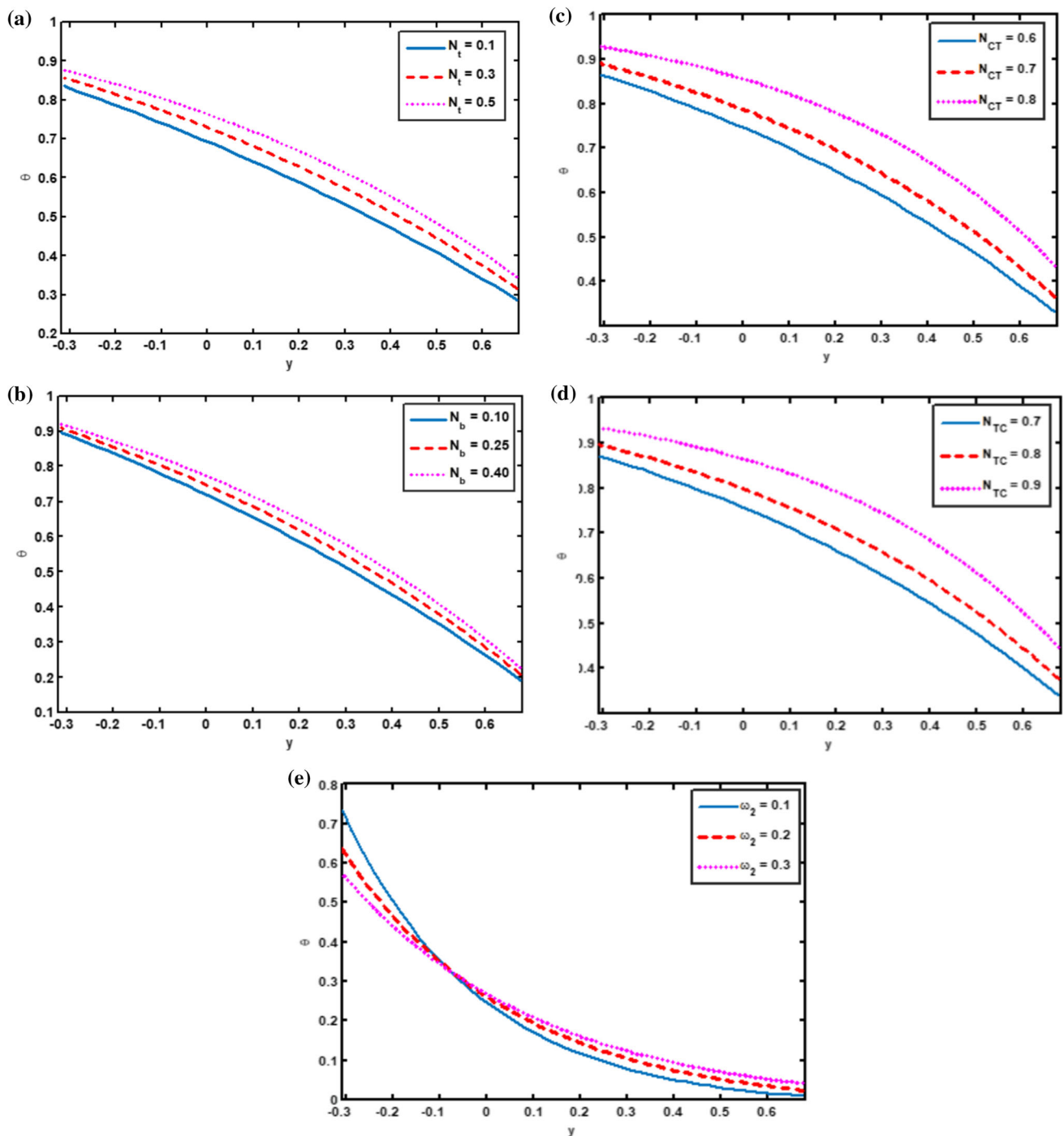


Fig. 2 Profile of temperature for N_t , N_b , N_{CT} , N_{TC} , and ω_2

This means that the flow can pass through without creating a significant pressure gradient. To keep the flux flowing through the narrow region of the channel $x \in [0.4, 0.6]$, a higher-pressure gradient is necessary. When the values of β , M and Wi are increased, the pressure gradient is observed to grow (Fig. 6a–c) but it reduces as the N_t values are increased (Fig. 6d). Figure 7a–f demonstrates the impact of velocity

on β , ω_1 , M , G_{rF} , N_t , and N_{TC} . It is noticed in Fig. 7a that when $y \in [0, 0.5]$ the magnitude of velocity decreases by increasing β values. Figure 7b shows that increasing M values decreases the magnitude of velocity for $y \in [-0.3, 0]$ and $y \in [0.55, 0.68]$, whereas increasing M values increases the magnitude of velocity when $y \in [0, 0.5]$. The velocity

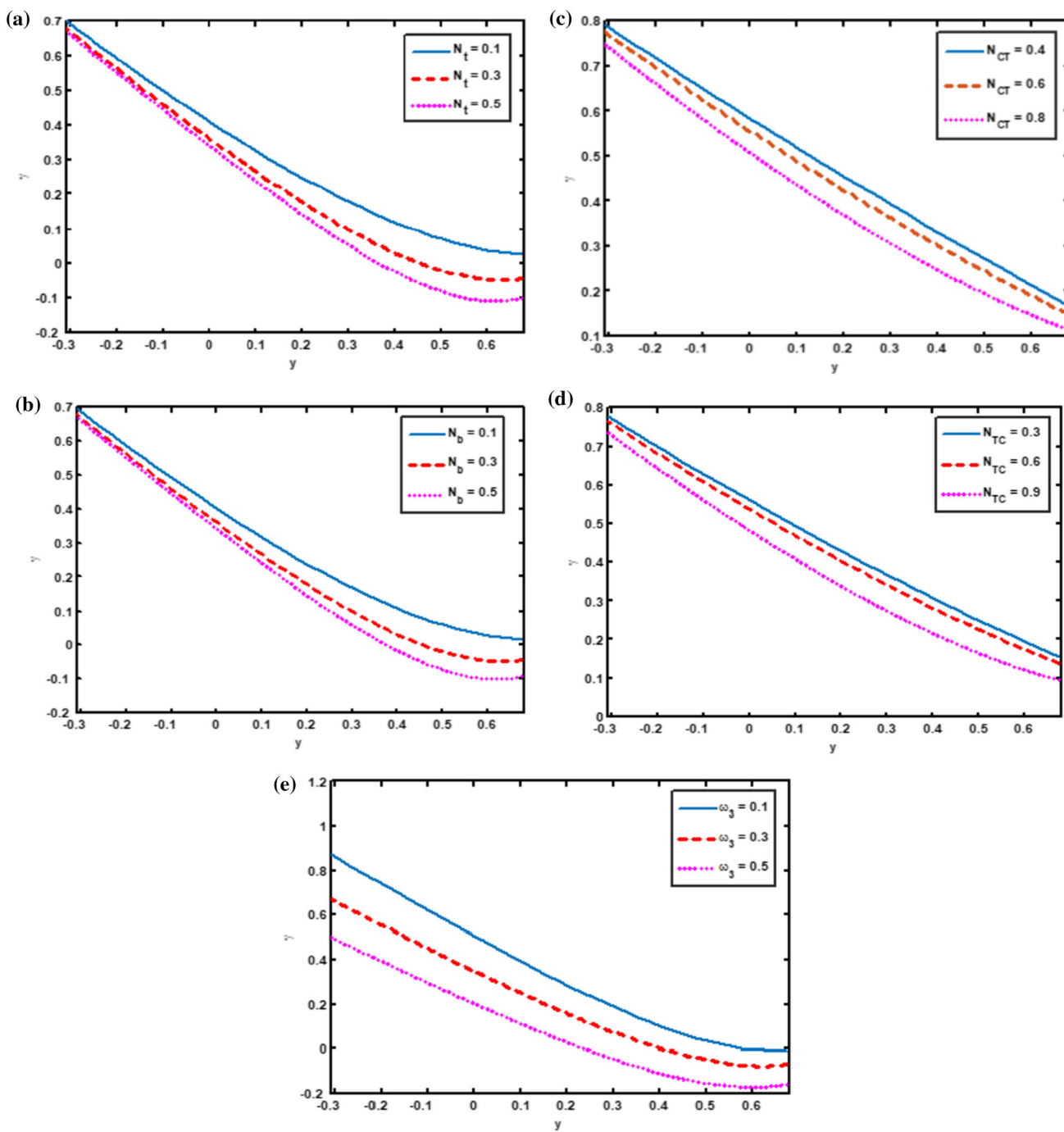


Fig. 3 Profile of concentration for N_t , N_b , N_{CT} , N_{TC} , and ω_3

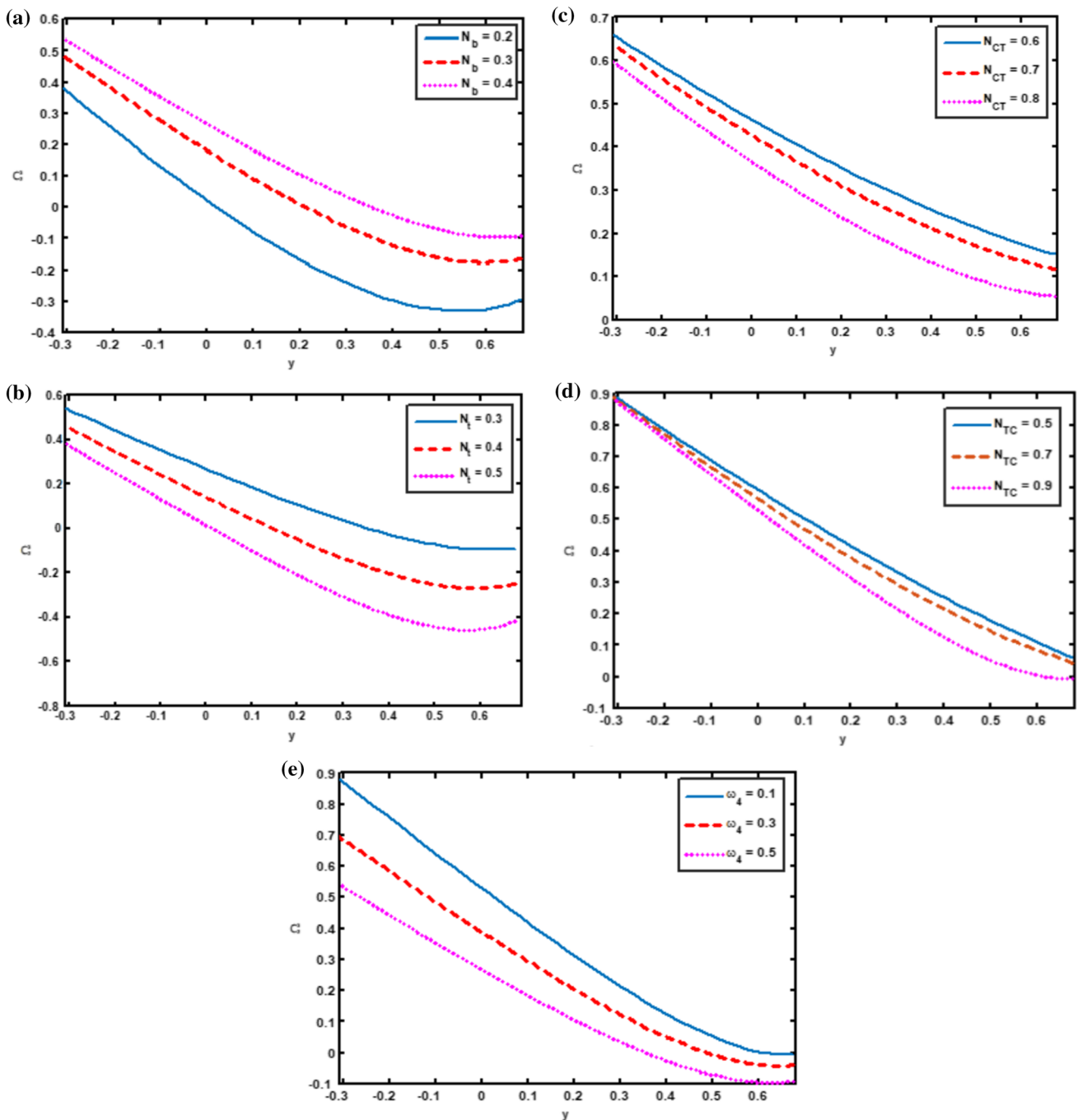


Fig. 4 Profile of nanoparticle fraction for N_b , N_t , N_{CT} , N_{TC} , and ω_4

at the walls is seen to be reduced as M increases. In reality, increasing the magnetic number increases the Lorentz force, which acts as a retarding force at the walls, reducing fluid speed. Figure 7c shows the effect of the slip parameter of velocity ω_1 . Figure 7c shows that increasing ω_1 values decreases the magnitude of velocity when $y \in [-0.3, -0.25]$ and $y \in [0.4, 0.68]$, whereas increasing ω_1 values increases the magnitude of velocity when $y \in [-0.25, 0.4]$. The slip

effect in the channel causes the fluid particles to stray, slowing the fluid velocity. The influence of G_{rF} , N_t , and N_{TC} on velocity is studied in Fig. 7d–f. The magnitude of velocity increases when $y \in [-0.3, 0.2]$ due to reduction in the drag force but reduces when $y \in [0.2, 0.85]$ by increasing G_{rF} , N_t , and N_{TC} .

Figures 8, 9, 10, and 11 are plotted to show the effect of streamlines. As shown in Fig. 8, increasing the velocity slip parameter ω_1 reduces the quantity of trapped boluses in

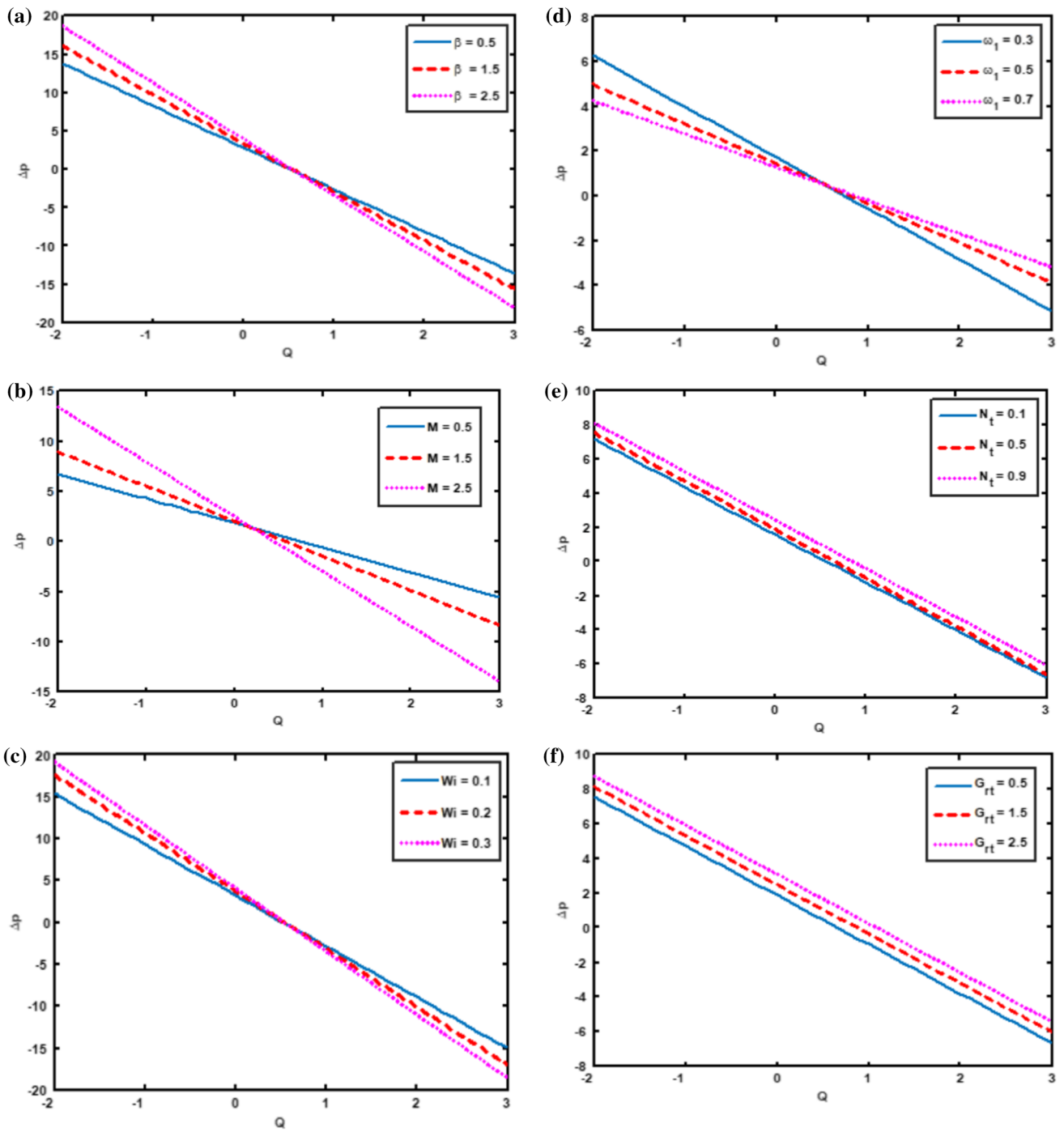


Fig. 5 Profile of pressure rise for β , M , Wi , ω_1 , N_t , and G_{rt}

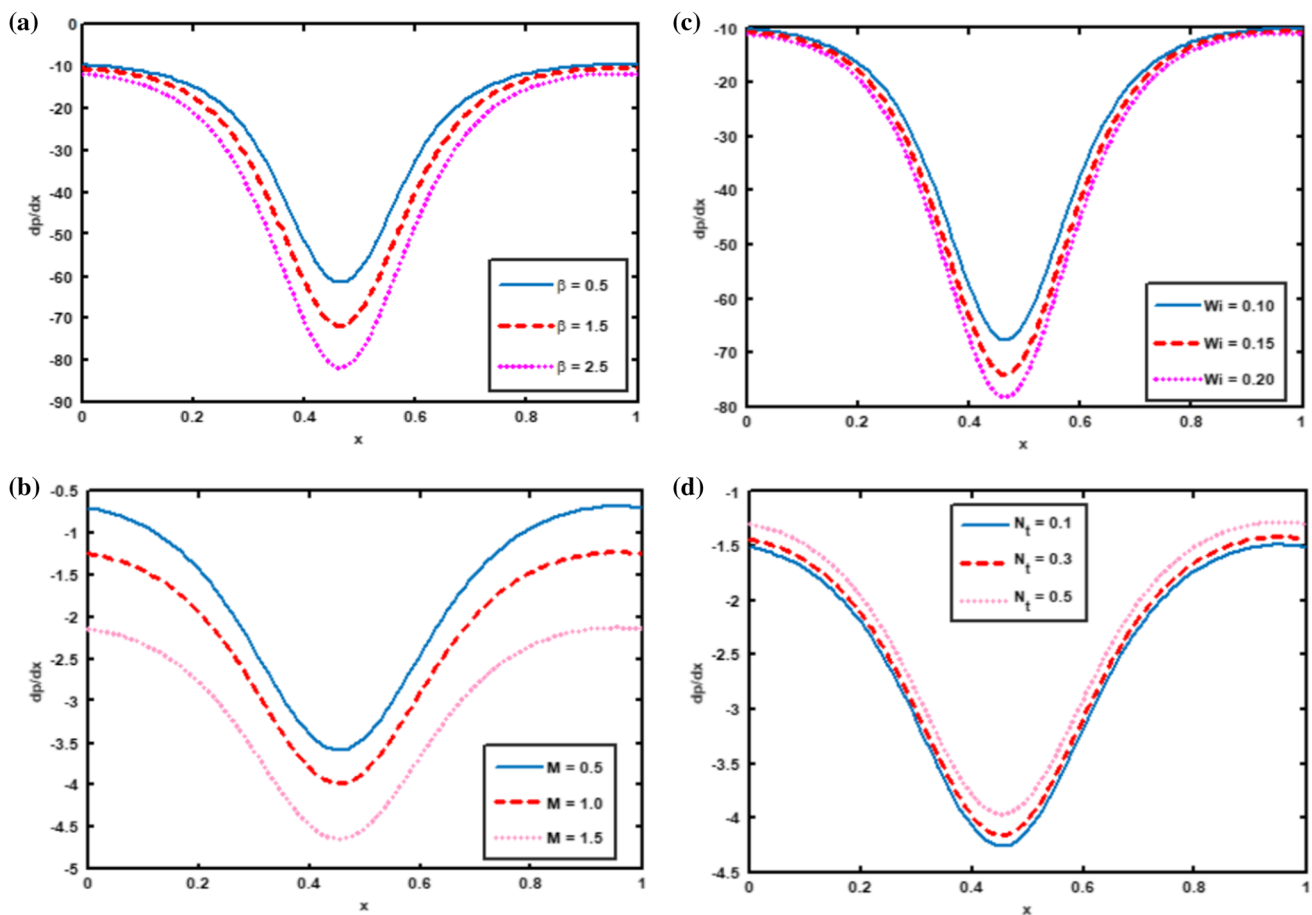


Fig. 6 Profile of pressure gradient for β , M , Wi , and N_t

both the top and lower parts of the channel. By raising N_{TC} and G_{rF} values, the quantity of trapped bolus grows in the upper part of the channel, while the size of trapped bolus increases in the lower section (Figs. 9 and 10). By raising the slip parameter of temperature ω_2 , the size of the trapped bolus decreases in the top half of the channel, while the size of the trapped bolus increases in the lower half of the channel (Fig. 11).

6 Concluding Remarks

This section provides a final remark on the ongoing problem. The primary purpose of a new study is to determine the importance and impacts of slip on double-diffusive convection flows. Numerical methodologies can be utilized to solve nonlinear equations, and graphical results can be employed to evaluate various embedded constraints. The major significant findings are as follows:

- The temperature profile increases when thermophoresis N_t and Brownian motion N_b parameters are enhanced. By

increasing N_t , nanoparticle concentration becomes higher which cause the temperature profiles to rise. Increasing N_b increases the average kinetic energy, and hence, it causes an increase in temperature profiles.

- The solutal concentration profile decreases by enhancing all the diffusion parameters, viz. thermophoresis N_t , Brownian motion N_b , Soret N_{CT} , and Dufour N_{TC} parameter. Also, solutal concentration profiles are found decreasing as slip parameter ω_3 intensifies.
- The density of nanoparticles fraction raises by increasing Brownian motion N_b because it increases the average kinetic energy and hence particles move it effects the motion of nano particles. However, opposite behavior is noted in the case of N_t , N_{CT} , N_{TC} , and ω_4 .
- The enhancement of slip effect ω_1 inside the channel for Johnson–Segalman nanofluids with double-diffusive effects is found flow resisting as it causes the fluid particles to stray, slowing the fluid velocity. However, opposite behavior is observed near the boundary wall of the channel.
- The velocity at the walls is seen to be enhanced as the Hartmann number M increases. This means that when

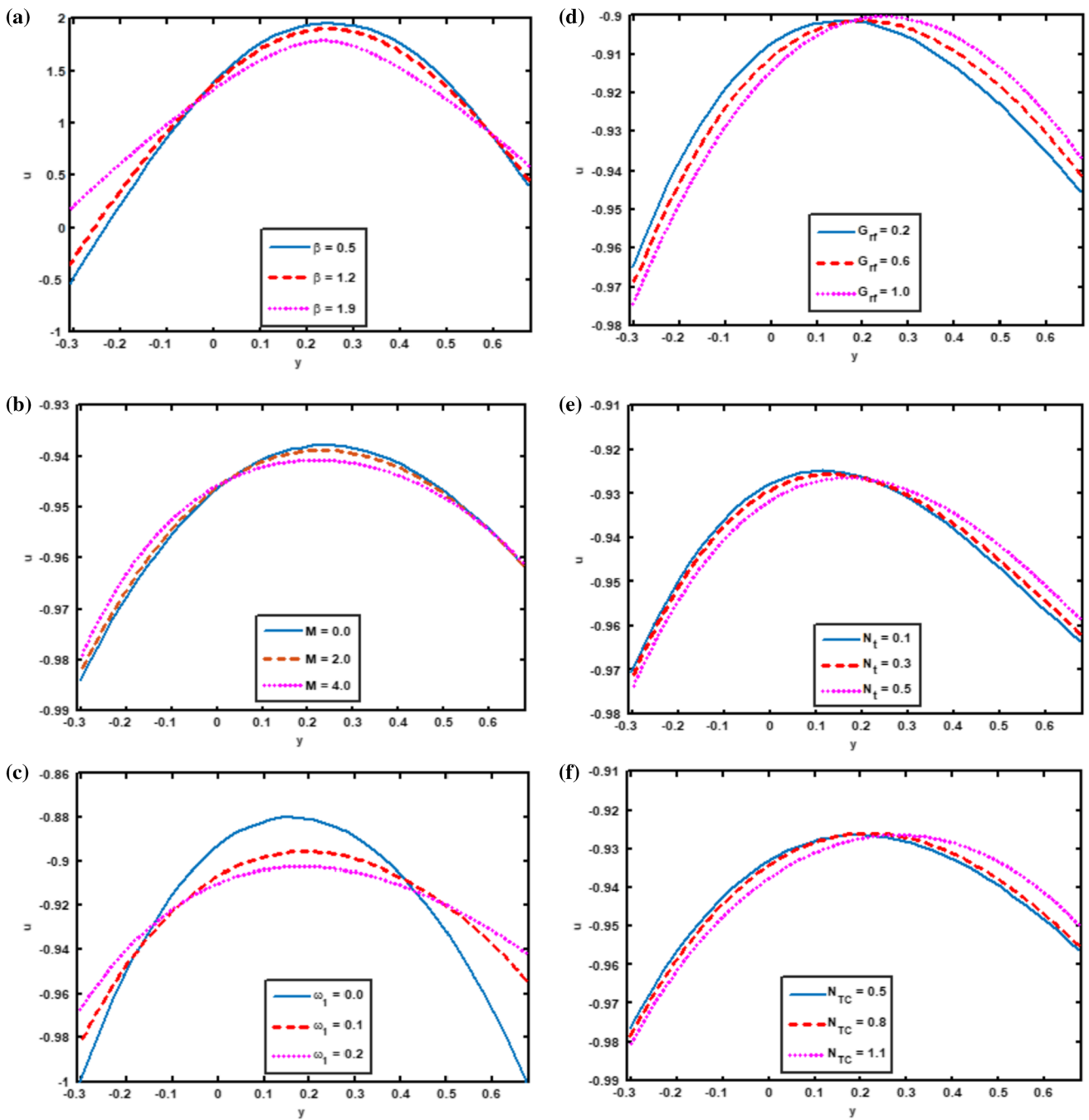


Fig. 7 Profile of velocity for β , M , ω_1 , G_{rF} , N_t , and N_{TC}

Fig. 8 Streamlines for ω_1

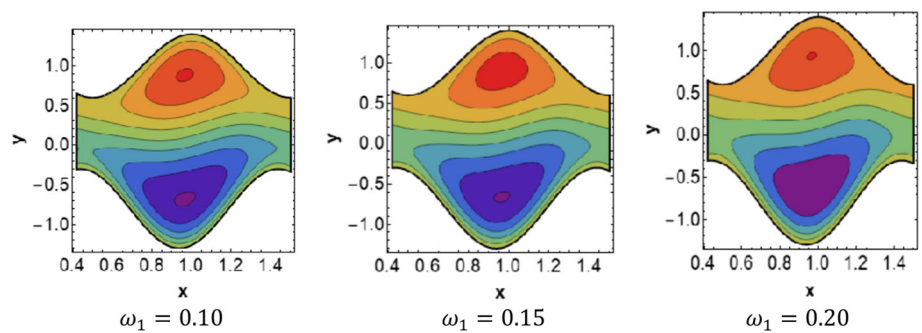


Fig. 9 Streamlines for N_{TC}

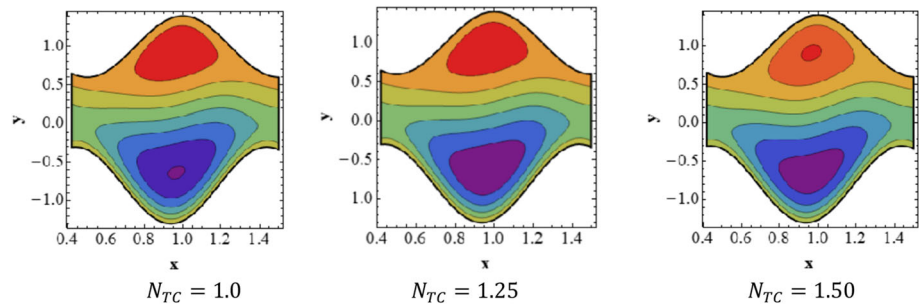


Fig. 10 Streamlines for G_{rF}

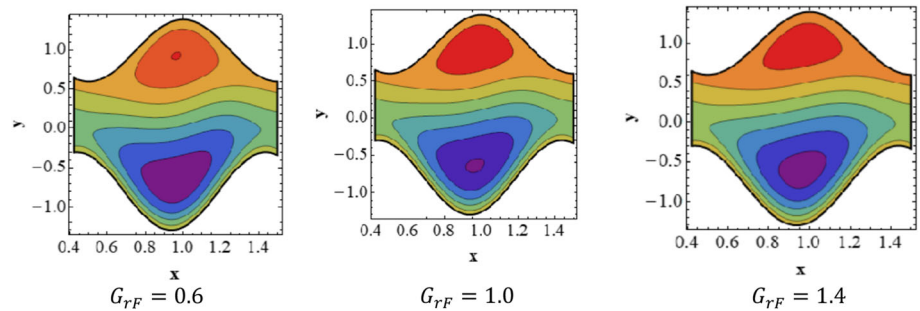
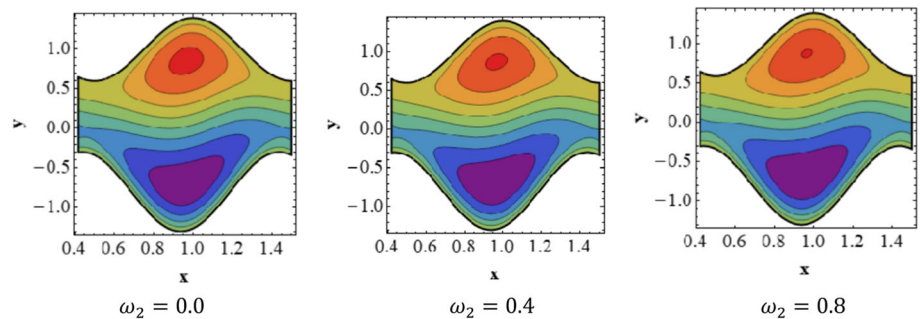


Fig. 11 Streamlines for ω_2



magnetic effects are dominating the viscous effects that speed of fluid near walls tends to increase.

- The volume of trapped bolus grows in the upper part of the channel as N_{TC} and G_{rF} values are increased, while the size of trapped bolus expands in the lower part.

Declarations

Conflict of interest The authors declare that they have no conflict of interest.

References

1. Bertuzzi, A.; Mancinelli, R.; Pescatori, M.; Salinari, S.; Ghista, D.N.: Models of gastrointestinal tract motility. In: Kline, J. (Ed.) Hand Book of Biomedical Engineering, pp. 637–654. Academic Press, London, UK (1988)
2. J. N. J. Lozano, Peristaltic flow with application to ureteral biomechanics, Ph.D. thesis, Aerospace and Mechanical Engineering, University of Notre Dame, Notre Dame, Ind, USA

3. Quillin, K.J.: Kinematic scaling of locomotion by hydrostatic animals: ontogeny of peristaltic crawling by the earthworm *Lumbricus terrestris*. *J. Exp. Biol.* **202**, 661–674 (1999)
4. Saga, N.; Nakamura, T.: Development of a peristaltic crawling robot using magnetic fluid on the basis of the locomotion mechanism of the earthworm. *Smart Mater. Struct.* **13**, 566–569 (2004)
5. T. W. Latham, Fluid motion in a peristaltic pump, M.Sc. Thesis, MIT, Cambridge, 1966.
6. Jaffrin, M.Y.; Shapiro, A.H.: Peristaltic pumping. *Annu. Rev. Fluid Mech.* **3**, 13–37 (1971)
7. Burns, J.C.; Parkes, J.: Peristaltic motion. *J. Fluid Mech.* **29**, 731–743 (1967)
8. Chow, T.S.: Peristaltic transport in a circular cylindrical pipe. *J. Appl. Mech.* **37**, 901–906 (1970)
9. Mishra, M.; Rao, A.R.: Peristaltic transport of a Newtonian fluid in an asymmetric channel. *Zeitschrift fur angewandte Mathematik and Physik* **54**, 532–550 (2004)
10. Shapiro, A.H.; Jaffrin, M.Y.; Weinberg, S.L.: Peristaltic pumping with long wavelengths at low Reynolds number. Cambridge University Press **37**, 799–825 (1969)
11. Takabatake, S.; Ayukawa, K.: Numerical study of two-dimensional peristaltic flows. *J. Fluid Mech.* **122**, 439–465 (1982)
12. Johnson, M.W., Jr.; Segalman, D.: A model for viscoelastic fluid behavior which allows non-affine deformation. *J. Nonnewton. Fluid Mech.* **2**, 255–270 (1977)

13. Malkus, D.S.; Nohel, J.A.; Plohr, B.J.: Dynamics of shear flows of non-Newtonian fluids. *J. Comput. Phys.* **87**, 464–497 (1990)
14. Vinogradov, G.V.; Malkin, A.Y.; Yanovskii, G.Y.; Borisenkova, E.K.; Yarlykov, B.V.; Brezhnava, G.V.: Viscoelastic properties and flow of narrow distribution polybutadienes and polyisoprenes. *J. Polym. Sci. Part A-2* **10**, 1061–1084 (1972)
15. McLeish, T.C.B.; Ball, R.C.: A molecular approach to the spurt effect in polymer melt flow. *J. Polym. Sci. (B)* **24**, 1765–1745 (1986)
16. Hayat, T.; Afsar, A.; Ali, N.: Peristaltic transport of a Johnson-Segalman fluid in an asymmetric channel. *Math. Comput. Model.* **47**, 380–400 (2008)
17. Kraynik, A.M.; Schowalter, W.R.: Slip at the wall and extrudate roughness with aqueous solutions of polyvinyl alcohol and sodium borate. *J. Rheol.* **25**, 95–114 (1981)
18. S. U. S. Choi, Enhancing thermal conductivity of fluids with nanoparticles. In: Proceedings of the ASME International Mechanical Engineering Congress and Exposition, San Francisco, CA, USA, (1995) 99–105 .
19. S. Mosayebidorcheh, M. Hatami Analytical investigation of peristaltic nanofluid flow and heat transfer in an asymmetric wavy wall channel, *International Journal of Heat and Mass Transfer*,
20. Akram, S.; Afzal, Q.: Effects of thermal and concentration convection and induced magnetic field on peristaltic flow of Williamson nanofluid in inclined uniform channel. *Eur. Phys. J. Plus* **135**, 857 (2020)
21. Ellahi, R.; Zeeshan, A.; Hussain, F.; Asadollahi, A.: Peristaltic blood flow of couple stress fluid suspended with nanoparticles under the influence of chemical reaction and activation energy. *Symmetry* **11**, 276 (2019)
22. Akram, S.; Nadeem, S.: Influence of nanoparticles phenomena on the peristaltic flow of pseudoplastic fluid in an inclined asymmetric channel with different wave forms. *Iran. J. Chem. Chem. Eng.* **36**, 107–124 (2017)
23. Prakash, J.; Tripathi, D.; Triwari, A.K.; Sait, S.M.; Ellahi, R.: Peristaltic pumping of nanofluids through tapered channel in porous environment: Applications in blood flow. *Symmetry* **11**, 868 (2019)
24. Kayani, S.M.; Hina, S.; Mustafa, M.: A new model and analysis for peristalsis of Carreau-Yasuda (CY) nanofluid subject to wall properties. *Arab. J. Sci. Eng.* **45**, 5179–5190 (2020)
25. Akbar, N.S.; Nadeem, S.: Endoscopic effects on the peristaltic flow of a nanofluid. *Commun. Theor. Phys.* **56**, 761–768 (2011)
26. Bhatti, M.M.; Zeeshan, A.; Ellahi, R.: Simultaneous effects of coagulation and variable magnetic field on peristaltically induced motion of Jeffrey nanofluid containing gyrotactic microorganism. *Microvasc. Res.* **110**, 32–42 (2017)
27. Qasim, M.; Ali, Z.; Wakif, A.; Boulahia, Z.: Numerical simulation of MHD peristaltic flow with variable electrical conductivity and Joule dissipation using generalized quadrature method. *Commun. Theor. Phys.* **71**, 509–518 (2019)
28. Ali, F.; Sheikh, N.A.; Khan, I.; Saqib, M.: Magnetic field effect on blood flow of Casson fluid in axisymmetric cylindrical tube: a fractional model. *J. Magn. Magn. Mater.* **423**, 327–336 (2017)
29. Tripathi, D.; Beg, O.: A study on peristaltic flow of nanofluids: application in drug delivery systems. *Int. J. Heat Mass Transf.* **70**, 61–70 (2014)
30. Sucharitha, G.; Vajravelu, K.; Lakshminarayana, P.: Magnetohydrodynamic nanofluid flow in a non-uniform aligned channel with Joule heating. *J. Nanofluids* **8**, 1373 (2019)
31. Kothandapani, M.; Prakash, J.: Effects of thermal radiation parameter and magnetic field on the peristaltic motion of Williamson nanofluid in a tapered asymmetric channel. *Int. J. Heat Mass Transf.* **81**, 234–245 (2015)
32. Reddy, M.G.; Makinde, O.D.: Magnetohydrodynamic peristaltic transport of Jeffrey nanofluid in an asymmetric channel. *J. Mol. Liq.* **223**, 1242–1248 (2016)
33. Raza, M.; Ellahi, R.; Sait, S.M.; Sarafraz, M.M.; Shadloo, M.S.; Waheed, I.: Enhancement of heat transfer in peristaltic flow in a permeable channel under induced magnetic field using different CNTs. *J. Therm. Anal. Calorim.* **140**, 1277–1291 (2019)
34. Akram, S.: Effects of nanofluid on peristaltic flow of a Carreau fluid model in an inclined magnetic field. *Heat Transf. Asian Res.* **43**, 368–383 (2014)
35. Raza, M.; Ellahi, R.; Sait, S.M.; Sarfaraz, M.M.; Shadloo, M.S.; Waheed, I.: Enhancement of heat transfer in peristaltic flow in a permeable channel under induced magnetic field using different CNTs. *J. Therm. Anal. Calorim.* **140**, 1277–1291 (2020)
36. Hussain, S.; Jamal, M.; Haddad, Z.; Arc, M.: Numerical modeling of magnetohydrodynamic thermosolutal free convection of power law fluids in a staggered porous enclosure. *Sustain. Energy Technol. Assess.* **53**, 102395 (2022)
37. Yildiz, Ç.; Arc, M.; Karabay, H.: Effect of inclination angle on natural convection of nanofluids in a U-shaped cavity. *Int. J. Environ. Sci. Technol.* **16**, 5289–5294 (2019)
38. Ali, F.H.; Hamzah, H.K.; Egab, K.; Arc, M.; Shahsavari, A.: Non-Newtonian nanofluid natural convection in a U-shaped cavity under magnetic field. *Int. J. Mech. Sci.* **186**, 105887 (2021)
39. Al-Amir, Q.R.; Hamzah, H.K.; Ali, F.H.; Bayraktar, S.; Arc, M.; Hatami, M.: Comparison study of vertical and horizontal elastic wall on vented square enclosure filled by nanofluid and hexagonal shape with MHD effect. *Eur. Phys. J. Special Top.* **231**, 2623–2643 (2022)
40. Yildiz, Ç.; Arc, M.; Karabay, H.; Bennacer, R.: Natural convection of nanofluid in a U-shaped enclosure emphasizing on the effect of cold rib dimensions. *J. Therm. Anal. Calorim.* **146**, 801–811 (2021)
41. Garimella, S.V.; Simpson, J.E.: Effect of thermo solutal convection on directional solidification. *Sadhana* **26**, 121–136 (2001)
42. Akbar, N.S.; Habib, M.B.: Peristaltic pumping with double diffusive natural convective nanofluid in a lopsided channel with accounting thermophoresis and Brownian moment. *Microsyst. Technol.* **25**, 1217–1226 (2019)
43. Sharma, A.; Tripathi, D.; Sharma, R.K.; Tiwari, A.K.: Analysis of double diffusive convection in electroosmosis regulated peristaltic transport of nanofluids. *Physica A* **535**, 122148 (2019)
44. Anwar Bég, O.; Tripathi, D.: Mathematica simulation of peristaltic pumping with double-diffusive convection in nanofluids a bio-nanoengineering model. *Proc. Inst. Mech. Eng. Part N* **225**, 99–114 (2012)
45. Akram, S.; Afzal, Q.; Aly, E.H.: Half-breed effects of thermal and concentration convection of peristaltic pseudoplastic nanofluid in a tapered channel with induced magnetic field. *Case Stud. Therm. Eng.* **22**, 100775 (2020)
46. Alolaiyan, H.; Riaz, A.; Razaq, A.; Saleem, N.; Zeeshan, A.; Bhatti, M.M.: Effects of double diffusion convection on third grade nanofluid through a curved compliant peristaltic channel. *Coatings* **10**(2), 154 (2020)
47. Asha, S.K.; Sunitha, G.: Thermal radiation and hall effects on peristaltic blood flow with double diffusion in the presence of nanoparticles. *Case Stud. Therm. Eng.* **17**, 100560 (2020)
48. Akram, S.; Athar, M.; Saeed, K.: Hybrid impact of thermal and concentration convection on peristaltic pumping of Prandtl nanofluids in non-uniform inclined channel and magnetic field. *Case Stud. Therm. Eng.* **25**, 100965 (2021)
49. Riaz, A.; Khan, S.U.D.; Zeeshan, A.; Khan, S.U.; Hassan, M.; Muhammad, T.: Thermal analysis of peristaltic flow of nanosized particles within a curved channel with second-order partial slip and porous medium. *J. Thermal Anal. Calorim.* **143**, 1997–2009 (2021)
50. Ali, A.; Saleem, S.; Mumraiz, S.; Saleem, A.; Awais, M.; Khan Marwat, D.N.: Investigation on TiO₂-Cu/H₂O hybrid nanofluid with slip conditions in MHD peristaltic flow of Jeffrey material. *J. Therm. Anal. Calorim.* **143**, 1985–1996 (2021)



51. Derek, C.; Tretheway, D.C.; Meinhart, C.D.: Apparent fluid slip at hydrophobic microchannel walls. *Phys. Fluids* **14**, L9–L12 (2002)
52. Akram, S.; Razia, A.; Afzal, F.: Effects of velocity second slip model and induced magnetic field on peristaltic transport of non-Newtonian fluid in the presence of double-diffusivity convection in nanofluids. *Arch. Appl. Mech.* **90**, 1583–1603 (2020)
53. Aly, E.H.; Ebaid, A.: Effect of the velocity second slip boundary condition on the peristaltic flow of nanofluids in an asymmetric channel: exact solution. *Abstr. Appl. Anal.* **2014**, 191876 (2014)
54. Hina, S.: MHD peristaltic transport of Eyring–Powell fluid with heat/mass transfer, wall properties and slip conditions. *J. Magn. Mater.* **404**, 148–158 (2016)

Springer Nature or its licensor (e.g. a society or other partner) holds exclusive rights to this article under a publishing agreement with the author(s) or other rightsholder(s); author self-archiving of the accepted manuscript version of this article is solely governed by the terms of such publishing agreement and applicable law.